

# SUSY Fits and their Implications for ILC and CLIC\*

S. HEINEMEYER<sup>1,2†</sup>

<sup>1</sup>*Instituto de Física Teórica, (UAM/CSIC), Universidad Autónoma de Madrid, Cantoblanco, E-28049 Madrid, Spain*

<sup>2</sup>*Instituto de Física de Cantabria (CSIC-UC), E-39005 Santander, Spain*

## Abstract

We review results from our frequentist analysis of the parameter space of the pMSSM10, in which the following 10 soft SUSY-breaking parameters are specified independently at the mean scalar top mass scale  $M_{\text{SUSY}} \equiv \sqrt{m_{\tilde{t}_1} m_{\tilde{t}_2}}$ : the gaugino masses  $M_{1,2,3}$ , the first- and second-generation squark masses  $m_{\tilde{q}_1} = m_{\tilde{q}_2}$ , the third-generation squark mass  $m_{\tilde{q}_3}$ , a common slepton mass  $m_{\tilde{\ell}}$  and a common trilinear mixing parameter  $A$ , as well as the Higgs mixing parameter  $\mu$ , the pseudoscalar Higgs mass  $M_A$  and  $\tan \beta$ , the ratio of the two Higgs vacuum expectation values. We implemented the LHC searches for strongly- and electroweakly-interacting sparticles and light stops, so as to confront the pMSSM10 parameter space with all relevant SUSY searches. In addition, our analysis includes Higgs mass and rate measurements, SUSY Higgs exclusion bounds, the measurements of  $\text{BR}(B_s \rightarrow \mu^+ \mu^-)$ , other  $B$ -physics observables, electroweak precision observables, the cold dark matter density and the searches for spin-independent dark matter scattering, assuming that the cold dark matter is mainly provided by the lightest neutralino  $\tilde{\chi}_1^0$ . We discuss the discovery potential of future  $e^+e^-$  linear colliders, such as ILC and CLIC, in the preferred pMSSM10 parameter space.

---

\* Talk (on behalf of the MasterCode collaboration) presented at the International Workshop on Future Linear Colliders (LCWS15), Whistler, Canada, 2-6 November 2015.

† email: Sven.Heinemeyer@cern.ch

# 1 Introduction

In order to confront the parameter space of the Minimal Supersymmetric Standard Model (MSSM) [1–3] with experimental data, one can take a purely phenomenological approach in which the soft SUSY-breaking parameters are specified at low energies, and are not required to be universal at any input scale, a class of models referred to as the phenomenological MSSM with  $n$  free parameters (pMSSM $n$ ) [4]. Here we review a recent exploration of this framework, the pMSSM10 [5, 6], in particular in view of the physics at a future  $e^+e^-$  linear collider, such as the ILC [7–10] or CLIC [10, 11].

In our version of the pMSSM10 the following assumptions are made. Motivated by the absence of significant flavor-changing neutral interactions (FCNI) beyond those in the Standard Model (SM), we assume that the soft SUSY-breaking contributions to the masses of the squarks of the first two generations are equal, which we also assume for the three generations of sleptons. The FCNI argument does not motivate any relation between the soft SUSY-breaking contributions to the masses of left- and right-handed sfermions, but here we assume for simplicity that they are equal. As a result, we consider the following 10 parameters in our analysis (where “mass” is here used as a synonym for a soft SUSY-breaking parameter, and the gaugino masses and trilinear couplings are taken to be real):

$$\begin{aligned}
 & 3 \text{ gaugino masses} : M_{1,2,3}, \\
 & 2 \text{ squark masses} : m_{\tilde{q}_1} = m_{\tilde{q}_2} \neq m_{\tilde{q}_3}, \\
 & 1 \text{ slepton mass} : m_{\tilde{\ell}}, \\
 & 1 \text{ trilinear coupling} : A, \\
 & \text{Higgs mixing parameter} : \mu, \\
 & \text{Pseudoscalar Higgs mass} : M_A, \\
 & \text{Ratio of vevs} : \tan \beta.
 \end{aligned} \tag{1}$$

All of these parameters are specified at a low renormalisation scale, the mean scalar top mass scale,  $M_{\text{SUSY}} \equiv \sqrt{m_{\tilde{t}_1} m_{\tilde{t}_2}}$ , close to that of electroweak symmetry breaking. More information about the scan of the pMSSM10 parameter space using the `MultiNest` [12] technique can be found in Ref. [5].

## 2 Our method

As discussed above we consider a ten-dimension subset (pMSSM10) of the full MSSM parameter space. The selected SUSY parameters were listed in Eq. (1), and the ranges of these parameters that we sample are shown in Table 1. We also indicate in the right column of this Table how we divide the ranges of most of these parameters into segments for the `MultiNest` sampling.

We calculate the observables that go into our likelihood evaluation using the `MasterCode` framework [5, 6, 13–18], which interfaces various public and private codes: `SoftSusy` 3.3.9 [19] for the spectrum, `FeynWZ` [20] for the electroweak precision observables, `FeynHiggs` 2.10.0 [21, 22] for the Higgs sector and  $(g-2)_\mu$ , `SuFla` [23], `SuperIso` [24] for the  $B$ -physics observables, `Micromegas` 3.2 [25] for the dark matter relic density, `SSARD` [26] for

Parameter	Range	Number of segments
$M_1$	(-1 , 1 ) TeV	2
$M_2$	( 0 , 4 ) TeV	2
$M_3$	(-4 , 4 ) TeV	4
$m_{\tilde{q}}$	( 0 , 4 ) TeV	2
$m_{\tilde{q}_3}$	( 0 , 4 ) TeV	2
$m_{\tilde{l}}$	( 0 , 2 ) TeV	1
$M_A$	( 0 , 4 ) TeV	2
$A$	(-5 , 5 ) TeV	1
$\mu$	(-5 , 5 ) TeV	1
$\tan \beta$	( 1 , 60)	1
Total number of boxes		128

**Table 1:** Ranges of the *pMSSM10* parameters sampled, together with the numbers of segments into which each range was divided, and the corresponding number of sample boxes.

the spin-independent cross-section  $\sigma_p^{\text{SI}}$ , `SDECAY 1.3b` [27] for calculating sparticle branching ratios, and `HiggsSignals 1.3.0` [28] and `HiggsBounds 4.2.0` [29] for calculating constraints on the Higgs sector. the codes are linked using the SUSY Les Houches Accord (SLHA) [30].

For many of these constraints, we follow very closely our previous implementations, which were summarized recently in Table 1 in [17]. Updates concerning  $\text{BR}(b \rightarrow s\gamma)$ ,  $\text{BR}(B_u \rightarrow \tau\nu_\tau)$ , Higgs boson masses and rates etc. can be found in Ref. [5].

Particular attention has been paid to correctly include the various SUSY searches at the LHC. As most of these searches have been interpreted by ATLAS and CMS only in simplified model frameworks, we have introduced supplementary procedures in order to apply these searches to the complicated sparticle spectrum content of a full SUSY model such as the *pMSSM10*. For this we consider three separate categories of particle mass constraints that arise from the LHC searches: a) generic constraints on coloured sparticles (gluinos and squarks), b) dedicated constraints on electroweakly-interacting gauginos, Higgsinos and sleptons, c) dedicated constraints on stop production in scenarios with compressed spectra. In the following we refer to the combination of all these constraints from direct SUSY searches as the LHC8 constraint, with sectors labelled as  $\text{LHC8}_{\text{col}}$ ,  $\text{LHC8}_{\text{EWK}}$ , and  $\text{LHC8}_{\text{stop}}$ , respectively. The implementation of these results have been validated with `Atom` [31] and `Scorpion` [32].

## 3 Predictions for the ILC and CLIC

### 3.1 The Best-Fit Point

We start with the discussion of the characteristics of the best-fit point, whose parameters are listed in Table 2. The best-fit spectrum is shown in Fig. 1, and its SLHA file [30] can be

Parameter	Best-Fit
$M_1$	170 GeV
$M_2$	170 GeV
$M_3$	2600 GeV
$m_{\tilde{q}}$	2880 GeV
$m_{\tilde{q}_3}$	4360 GeV
$m_{\tilde{t}}$	440 GeV
$M_A$	2070 GeV
$A$	790 GeV
$\mu$	550 GeV
$\tan \beta$	37.6

**Table 2:** Parameters of the pMSSM10 best-fit point.

downloaded from the MasterCode website [18]. We note first the near-degeneracy between the  $\tilde{\chi}_1^0, \tilde{\chi}_2^0$  and  $\tilde{\chi}_1^\pm$ , which is a general feature of our 68% CL region that occurs in order to bring the cold dark matter density into the range allowed by cosmology. Correspondingly, we see in Table 2 that  $M_1 \simeq M_2$ , though  $M_3$  is very different. The overall  $\tilde{\chi}_1^0/\tilde{\chi}_2^0/\tilde{\chi}_1^\pm$  mass scale is bounded from below by the LEP and LHC8<sub>EWK</sub> constraints, and from above by  $(g-2)_\mu$ , especially at the 68% CL. We display in Fig. 2 the 95% (68%) CL intervals in our fit for the masses of pMSSM10 particles as lighter (darker) peach shaded bars, with the best-fit values being indicated with blue horizontal lines. Turning back to Fig. 1, we note the near-degeneracy between the slepton masses, which reflects our assumption of a common input slepton mass at the input scale  $M_{\text{SUSY}}$  that would not hold in more general versions of the pMSSM. The overall slepton mass scale is below 1 TeV, as seen in Fig. 2, being bounded from above by  $(g-2)_\mu$  and from below by LHC8<sub>EWK</sub> constraint. The latter also provides the strongest upper bound on the  $\tilde{\chi}_1^0/\tilde{\chi}_2^0/\tilde{\chi}_1^\pm$ . We also see in Fig. 2 that the gluino, squark, stop and bottom masses are all very poorly constrained in our pMSSM10 analysis, though the LHC8<sub>col</sub> constraint forbids low masses.

Concerning the Higgs sector, we note that the best-fit value for  $M_A$  lies in the multi-TeV region (where its actual value is only weakly constrained) and is therefore far in the decoupling region. Accordingly, the properties of the light Higgs boson at about 125 GeV resemble very closely those of the Higgs boson of the SM.

SUSY particle pair production at an  $e^+e^-$  collider is possible for masses up to  $\sqrt{s}/2$ , i.e. up to  $\sim 500$  GeV at the ILC and up to  $\sim 1500$  GeV at CLIC. Here it should be kept in mind that also the production of two different SUSY particles could be possible, such as  $e^+e^- \rightarrow \tilde{\chi}_1^0\tilde{\chi}_2^0$  or  $e^+e^- \rightarrow \tilde{\mu}_1\tilde{\mu}_2$ , thus extending the mass reach. From Fig. 2 it becomes obvious that in particular the electroweak sector of the pMSSM10 could be accessible at ILC or CLIC. This offers interesting prospects for the precision determination of the underlying SUSY parameters, see, e.g., Ref. [10]. In the next two subsections we review some more details on the preferred SUSY particle mass ranges as well as on the  $e^+e^-$  production cross sections for electroweak particles.

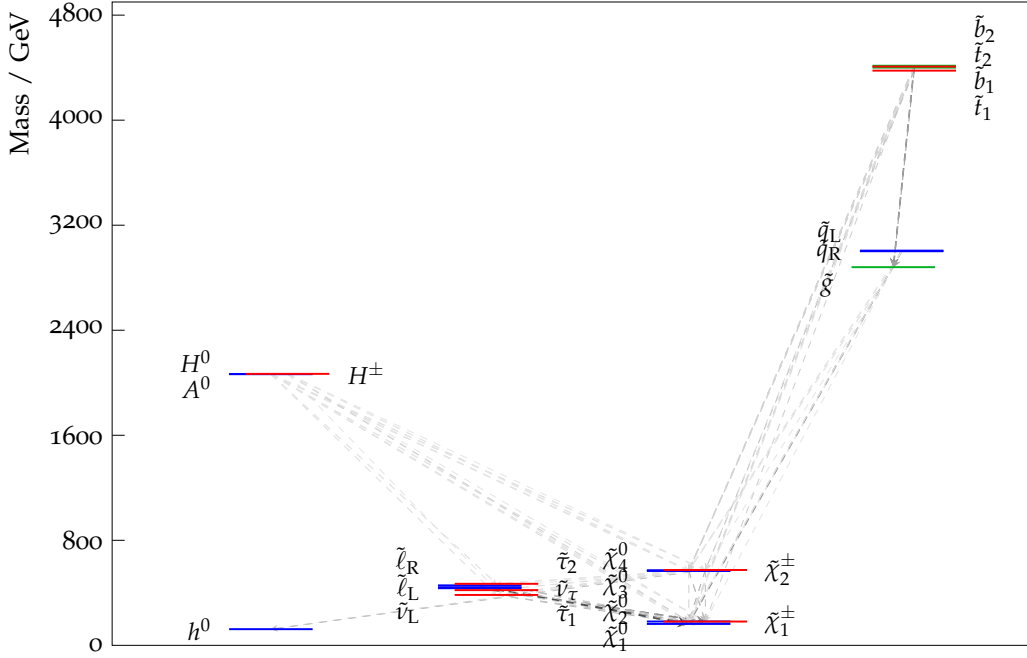


**Figure 1:** the particle spectrum and dominant decay branching ratios at our best-fit  $p\text{MSSM10}$  point. Note the near-degeneracies between  $\tilde{\chi}_1^0, \tilde{\chi}_2^0$  and  $\tilde{\chi}_1^\pm$ , between the sleptons, between  $\tilde{\chi}_3^0, \tilde{\chi}_4^0$  and  $\tilde{\chi}_2^\pm$ , between the  $\tilde{q}_L$  and  $\tilde{q}_R$ , between the heavy Higgs bosons, and between the stops and bottoms, which are general features of our 68% CL region. On the other hand, the overall sparticle mass scales, in particular of the coloured sparticles, are poorly determined.

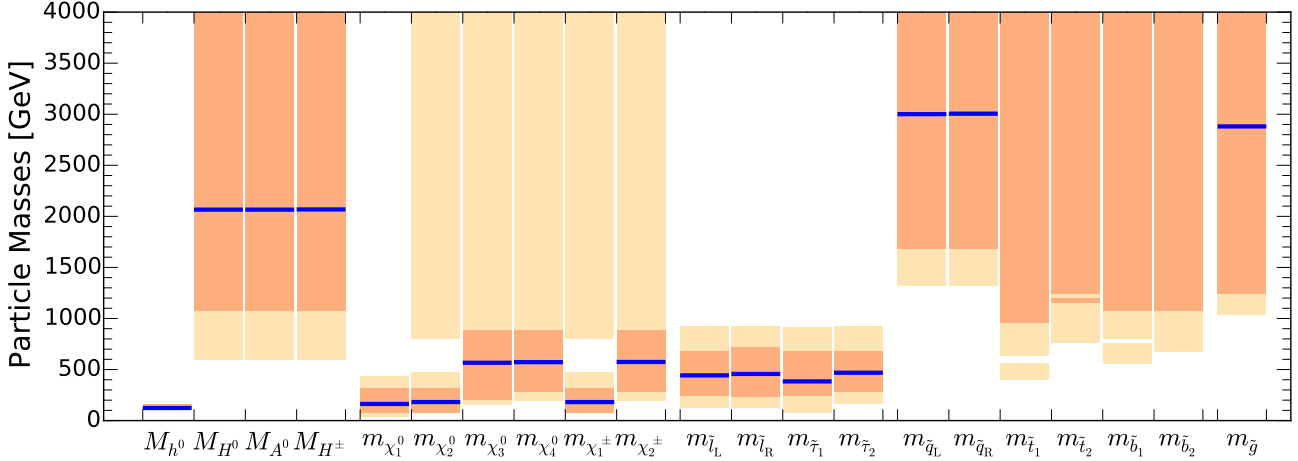


**Figure 2:** Summary of mass ranges predicted in the  $p\text{MSSM10}$ . the light (darker) peach shaded bars indicate the 95% (68%) CL intervals, whereas the blue horizontal lines mark the values of the masses at the best-fit point.

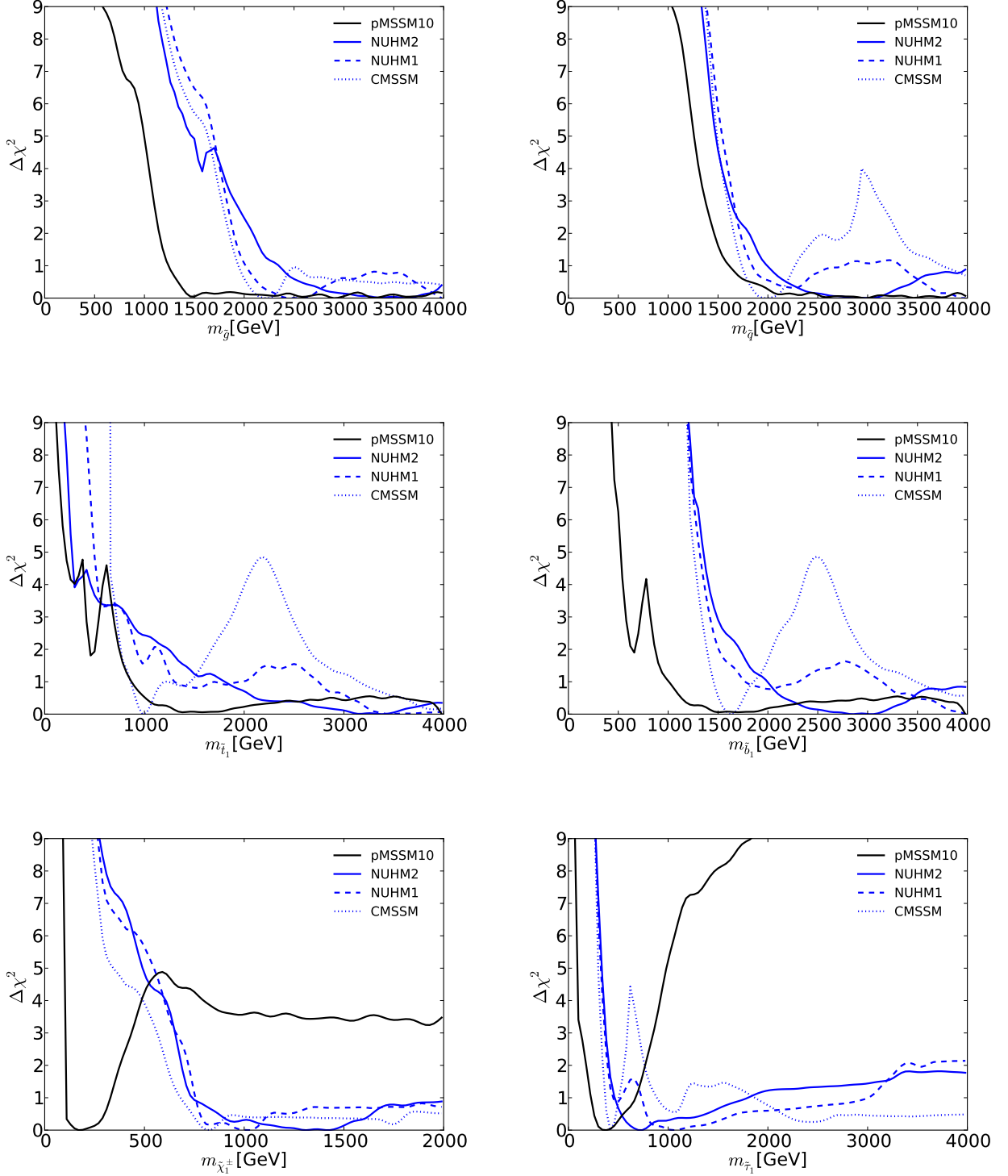
### 3.2 Sparticle Masses

Fig. 3 displays (from top left to bottom right) the one-dimensional profile likelihood functions for the masses of the gluino, the first- and second-generation squarks, the lighter stop and sbottom squarks, the lighter chargino and the lighter stau. In each panel the solid black line is for the pMSSM10, the solid blue line for the NUHM2, the dashed blue line for the NUHM1 and the dotted blue line for the CMSSM (the latter three lines are updated from Ref. [17] to include new constraints such as the LHC combined value of  $M_h$  [33]). In the case of  $m_{\tilde{g}}$ , we see that significantly lower masses are allowed in the pMSSM10 than in the other models:  $> 1250$  GeV at the 68% CL and  $\sim 1000$  GeV at the 95% CL. We also see that there is a similar, though smaller, reduction in the lower limit on  $m_{\tilde{q}}$ , to  $\sim 1500$  GeV at the 68% CL and  $\sim 1300$  GeV at the 95% CL. The picture is more complicated for  $m_{\tilde{t}_1}$ , where we see structures in the one-dimensional likelihood function for  $m_{\tilde{t}_1} < 1000$  GeV that are allowed at the 95% CL. This reflects the compressed stop spectra, see Ref. [5] for more details. In the bottom row of Fig. 3, the one-dimensional profile likelihood functions for  $m_{\tilde{\chi}_1^\pm}$  and  $m_{\tilde{\tau}_1}$  in the pMSSM have minima at the lower mass limits  $\sim 100$  GeV established at LEP, and there is an upper limit  $m_{\tilde{\tau}_1} \lesssim 1000$  GeV at the 95% CL. These effects are due to the  $(g-2)_\mu$  constraint and the choice of generation-independent slepton masses in the pMSSM10. On the other hand, the light chargino (which is nearly degenerate in mass with the second lightest neutralino) has an upper mass limit below 500 GeV at the 90%, which would allow neutralino and chargino pair production at an 1000 GeV  $e^+e^-$  collider, as we discuss below. However, we find no upper limit on  $m_{\tilde{\chi}_1^\pm}$  at the 95% CL.

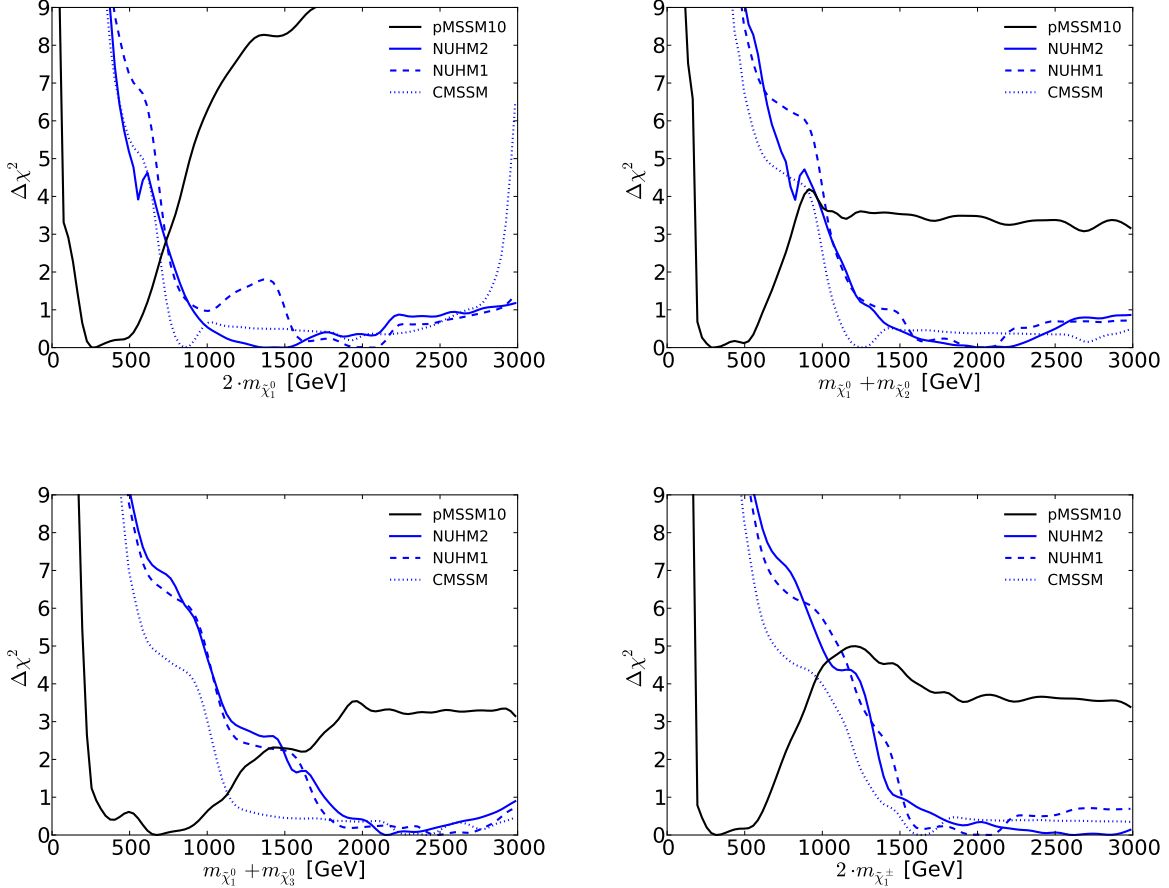
### 3.3 Prospects for Sparticle Detection at the ILC and CLIC

Fig. 4 displays the one-dimensional  $\chi^2$  functions for the lowest particle pair- and associated chargino and neutralino production thresholds in  $e^+e^-$  annihilation in the pMSSM10 (black), compared with their counterparts in the CMSSM (dotted blue), NUHM1 (dashed blue) and NUHM2 (solid blue). In the cases of  $\tilde{\chi}_1^0\tilde{\chi}_1^0$  (upper left panel),  $\tilde{\chi}_1^0\tilde{\chi}_2^0$  (upper right panel) and  $\tilde{\chi}_1^\pm\tilde{\chi}_1^\mp$  (lower right panel) production, we see that the minima of the  $\chi^2$  functions in the pMSSM10 lie within reach of an  $e^+e^-$  collider with centre-of-mass energy 500 GeV, and that threshold locations favoured by  $\Delta\chi^2 \leq 3$  would be within reach of a 1000 GeV collider, whereas no upper limit can be established at the 95% CL. We also see that, in the case of  $\tilde{\chi}_1^0\tilde{\chi}_3^0$  production (lower left panel) (which is very similar to the cases of  $\tilde{\chi}_1^0\tilde{\chi}_4^0$ ,  $\tilde{\chi}_2^0\tilde{\chi}_3^0$  and  $\tilde{\chi}_1^\pm\tilde{\chi}_2^\mp$  production that we do not show) the minimum of the global  $\chi^2$  function for the threshold lies between 400 GeV and 1000 GeV, again with no upper limit at the 95% CL. Referring back to the bottom right panel of Fig. 3, we see that slepton pair-production thresholds may well also lie below 1000 GeV. In all cases, the expected locations of the thresholds in the CMSSM, NUHM1 and NUHM2 are at much higher centre-of-mass energies.

Thus, the accessibility of supersymmetric particles at  $e^+e^-$  colliders is vastly different in the pMSSM10 and similar non-GUT models, as compared to the simplest GUT-based models. The prospects to produce SUSY particles at the ILC and CLIC are substantially better in the pMSSM10 than in the CMSSM, NUHM1 and NUHM2.



**Figure 3:** the one-dimensional profile likelihood functions for  $m_{\tilde{g}}$ ,  $m_{\tilde{q}}$ ,  $m_{\tilde{t}_1}$ ,  $m_{\tilde{b}_1}$ ,  $m_{\tilde{\chi}_1^\pm}$  and  $m_{\tilde{\tau}_1}$ . In each panel the solid black line is for the pMSSM10, the solid blue line for the NUHM2, the dashed blue line for the NUHM1 and the dotted blue line for the CMSSM.



**Figure 4:** the one-dimensional profile likelihood functions for various thresholds in  $e^+e^-$  annihilation. Upper left panel: the threshold for  $\tilde{\chi}_1^0\tilde{\chi}_1^0$  production. Upper right panel: the threshold for associated  $\tilde{\chi}_1^0\tilde{\chi}_2^0$  production. Lower left panel: the threshold for associated  $\tilde{\chi}_1^0\tilde{\chi}_3^0$  production. Lower right panel: the threshold for  $\tilde{\chi}_1^\pm\tilde{\chi}_1^\mp$  production.

## 4 Conclusions

We have reviewed the first global likelihood analysis of the pMSSM using a frequentist approach that includes comprehensive treatments of the LHC8 constraints, performed with the **MasterCode** framework. We have analysed the preferred mass ranges for SUSY particles and compared them to the reach of the ILC and CLIC. In particular, such a machine would have a significant discovery potential in the preferred region for the lighter neutralinos and charginos, as well as for scalar leptons, while those states would be difficult to access at the LHC (with the searches discussed in Ref. [5]).

## Acknowledgements

We thank E. Bagnaschi, O. Buchmueller, R. Cavanaugh, M. Citron, A. De Roeck, M. Dolan, J. Ellis, H. Flächer, G. Isidori, S. Malik, J. Marrouche, D. Martínez Santos, K. Olive, K. Sakurai, K. de Vries and G. Weiglein for the collaboration on the work presented here. The work of S.H. is supported in part by CICYT (grant FPA 2013-40715-P) and by the



## References

- [1] H. Nilles, Phys. Rept. **110** (1984) 1; R. Barbieri, Riv. Nuovo Cim. **11** (1988) 1.
- [2] H. Haber, G. Kane, Phys. Rept. **117** (1985) 75.
- [3] J. Gunion, H. Haber, Nucl. Phys. **B 272** (1986) 1.
- [4] See, for example, C. F. Berger, J. S. Gainer, J. L. Hewett and T. G. Rizzo, JHEP **0902**, 023 (2009) [arXiv:0812.0980 [hep-ph]]; S. S. AbdusSalam, B. C. Allanach, F. Quevedo, F. Feroz and M. Hobson, Phys. Rev. D **81**, 095012 (2010) [arXiv:0904.2548 [hep-ph]]; J. A. Conley, J. S. Gainer, J. L. Hewett, M. P. Le and T. G. Rizzo, Eur. Phys. J. C **71**, 1697 (2011) [arXiv:1009.2539 [hep-ph]]; J. A. Conley, J. S. Gainer, J. L. Hewett, M. P. Le and T. G. Rizzo, [arXiv:1103.1697 [hep-ph]]; B. C. Allanach, A. J. Barr, A. Dafinca and C. Gwenlan, JHEP **1107**, 104 (2011) [arXiv:1105.1024 [hep-ph]]; S. Sekmen, S. Kraml, J. Lykken, F. Moortgat, S. Padhi, L. Pape, M. Pierini and H. B. Prosper *et al.*, JHEP **1202** (2012) 075 [arXiv:1109.5119 [hep-ph]]; A. Arbey, M. Battaglia and F. Mahmoudi, Eur. Phys. J. C **72** (2012) 1847 [arXiv:1110.3726 [hep-ph]]; A. Arbey, M. Battaglia, A. Djouadi and F. Mahmoudi, Phys. Lett. B **720** (2013) 153 [arXiv:1211.4004 [hep-ph]]; M. W. Cahill-Rowley, J. L. Hewett, A. Ismail and T. G. Rizzo, Phys. Rev. D **88** (2013) 3, 035002 [arXiv:1211.1981 [hep-ph]]; C. Streve, G. Bertone, G. J. Besjes, S. Caron, R. Ruiz de Austri, A. Strubig and R. Trotta, JHEP **1409** (2014) 081 [arXiv:1405.0622 [hep-ph]]; M. Cahill-Rowley, J. L. Hewett, A. Ismail and T. G. Rizzo, Phys. Rev. D **91** (2015) 5, 055002 [arXiv:1407.4130 [hep-ph]]; L. Roszkowski, E. M. Sessolo and A. J. Williams, JHEP **1502**, 014 (2015) [arXiv:1411.5214 [hep-ph]]; M. E. C. Catalan, S. Ando, C. Weniger and F. Zandanel, arXiv:1503.00599 [hep-ph]; J. Chakraborty, A. Choudhury and S. Mondal, arXiv:1503.08703 [hep-ph].
- [5] K. J. de Vries *et al.*, Eur. Phys. J. C **75** (2015) 9, 422 [arXiv:1504.03260 [hep-ph]].
- [6] E. A. Bagnaschi *et al.*, Eur. Phys. J. C **75** (2015) 500 [arXiv:1508.01173 [hep-ph]].
- [7] H. Baer *et al.*, *The International Linear Collider Technical Design Report - Volume 2: Physics*, arXiv:1306.6352 [hep-ph].
- [8] TESLA Technical Design Report [TESLA Collaboration] Part 3, *Physics at an  $e^+e^-$  Linear Collider*, arXiv:hep-ph/0106315,  
see: [tesla.desy.de/new\\_pages/TDR\\_CD/start.html](http://tesla.desy.de/new_pages/TDR_CD/start.html) ;  
K. Ackermann *et al.*, DESY-PROC-2004-01.
- [9] J. Brau *et al.* [ILC Collaboration], *ILC Reference Design Report Volume 1 - Executive Summary*, arXiv:0712.1950 [physics.acc-ph];  
G. Aarons *et al.* [ILC Collaboration], *International Linear Collider Reference Design Report Volume 2: Physics at the ILC*, arXiv:0709.1893 [hep-ph].
- [10] G. Moortgat-Pick *et al.*, Eur. Phys. J. C **75** (2015) 8, 371 [arXiv:1504.01726 [hep-ph]].

- [11] L. Linssen, A. Miyamoto, M. Stanitzki and H. Weerts, arXiv:1202.5940 [physics.ins-det]; H. Abramowicz *et al.* [CLIC Detector and Physics Study Collaboration], *Physics at the CLIC  $e^+e^-$  Linear Collider – Input to the Snowmass process 2013*, arXiv:1307.5288 [hep-ex].
- [12] F. Feroz and M.P. Hobson, Mon. Not. Roy. Astron. Soc. **384** (2008) 449 [arXiv:0704.3704 [astro-ph]]. F. Feroz, M.P. Hobson and M. Bridges, Mon. Not. Roy. Astron. Soc. **398** (2009) 1601-1614 [arXiv:0809.3437 [astro-ph]]. F. Feroz, M.P. Hobson, E. Cameron and A.N. Pettitt, [arXiv:1306.2144 [astro-ph]].
- [13] O. Buchmueller *et al.*, Eur. Phys. J. C **72** (2012) 1878 [arXiv:1110.3568 [hep-ph]].
- [14] O. Buchmueller *et al.*, Eur. Phys. J. C **72** (2012) 2243 [arXiv:1207.7315].
- [15] O. Buchmueller *et al.*, Eur. Phys. J. C **74** (2014) 2809 [arXiv:1312.5233 [hep-ph]].
- [16] O. Buchmueller *et al.*, Eur. Phys. J. C **74** (2014) 2922 [arXiv:1312.5250 [hep-ph]].
- [17] O. Buchmueller *et al.*, Eur. Phys. J. C **74** (2014) 12, 3212 [arXiv:1408.4060 [hep-ph]].
- [18] For more information and updates, please see <http://cern.ch/mastercode/>.
- [19] B. C. Allanach, Comput. Phys. Commun. **143** (2002) 305 [arXiv:hep-ph/0104145].
- [20] S. Heinemeyer *et al.*, JHEP **0608** (2006) 052 [arXiv:hep-ph/0604147]; S. Heinemeyer, W. Hollik, A. M. Weber and G. Weiglein, JHEP **0804** (2008) 039 [arXiv:0710.2972 [hep-ph]].
- [21] G. Degrandi, S. Heinemeyer, W. Hollik, P. Slavich and G. Weiglein, Eur. Phys. J. C **28** (2003) 133 [arXiv:hep-ph/0212020]; S. Heinemeyer, W. Hollik and G. Weiglein, Eur. Phys. J. C **9** (1999) 343 [arXiv:hep-ph/9812472]; S. Heinemeyer, W. Hollik and G. Weiglein, Comput. Phys. Commun. **124** (2000) 76 [arXiv:hep-ph/9812320]; M. Frank *et al.*, JHEP **0702** (2007) 047 [arXiv:hep-ph/0611326]; See <http://www.feynhiggs.de>.
- [22] T. Hahn, S. Heinemeyer, W. Hollik, H. Rzehak and G. Weiglein, Phys. Rev. Lett. **112** (2014) 141801 [arXiv:1312.4937 [hep-ph]].
- [23] G. Isidori and P. Paradisi, Phys. Lett. B **639** (2006) 499 [arXiv:hep-ph/0605012]; G. Isidori, F. Mescia, P. Paradisi and D. Temes, Phys. Rev. D **75** (2007) 115019 [arXiv:hep-ph/0703035], and references therein.
- [24] F. Mahmoudi, Comput. Phys. Commun. **178** (2008) 745 [arXiv:0710.2067 [hep-ph]]; Comput. Phys. Commun. **180** (2009) 1579 [arXiv:0808.3144 [hep-ph]]; D. Eriksson, F. Mahmoudi and O. Stal, JHEP **0811** (2008) 035 [arXiv:0808.3551 [hep-ph]].
- [25] G. Belanger, F. Boudjema, A. Pukhov and A. Semenov, Comput. Phys. Commun. **176** (2007) 367 [arXiv:hep-ph/0607059]; Comput. Phys. Commun. **149** (2002) 103 [arXiv:hep-ph/0112278]; Comput. Phys. Commun. **174** (2006) 577 [arXiv:hep-ph/0405253].

- [26] Information about this code is available from K. A. Olive: it contains important contributions from T. Falk, A. Ferstl, G. Ganis, A. Mustafayev, J. McDonald, F. Luo, K. A. Olive, P. Sandick, Y. Santoso, V. Spanos, and M. Srednicki.
- [27] M. Muhlleitner, A. Djouadi, Y. Mambrini, *Comput. Phys. Commun.* **168** (2005) 46 [arXiv:hep-ph/0311167].
- [28] P. Bechtle, S. Heinemeyer, O. Stål, T. Stefaniak and G. Weiglein, *Eur. Phys. J. C* **74** (2014) 2, 2711 [arXiv:1305.1933 [hep-ph]]; *JHEP* **1411** (2014) 039 [arXiv:1403.1582 [hep-ph]].
- [29] P. Bechtle, O. Brein, S. Heinemeyer, G. Weiglein and K. E. Williams, *Comput. Phys. Commun.* **181** (2010) 138 [arXiv:0811.4169 [hep-ph]], *Comput. Phys. Commun.* **182** (2011) 2605 [arXiv:1102.1898 [hep-ph]]; P. Bechtle *et al.*, *Eur. Phys. J. C* **74** (2014) 3, 2693 [arXiv:1311.0055 [hep-ph]]; P. Bechtle, S. Heinemeyer, O. Stål, T. Stefaniak and G. Weiglein, *Eur. Phys. J. C* **75** (2015) 9, 421 [arXiv:1507.06706 [hep-ph]].
- [30] P. Skands *et al.*, *JHEP* **0407** (2004) 036 [arXiv:hep-ph/0311123]; B. Allanach *et al.*, *Comput. Phys. Commun.* **180** (2009) 8 [arXiv:0801.0045 [hep-ph]].
- [31] M. Papucci, K. Sakurai, A. Weiler and L. Zeune, *Atom: Automated Tests of Models, in preparation*.
- [32] *Scorpion* was first developed by J. Marrouche, and developed further by O. Buchmueller, M. Citron, S. Malik and K.J. de Vries: details may be obtained by contacting O. Buchmueller.
- [33] G. Aad *et al.* [CMS Collaboration], arXiv:1503.07589 [hep-ex].